

simulations are not accurate enough as yet to predict with confidence the consequences of protein replacement, but they may well be valuable in suggesting which mutations may have the most interesting consequences on enzyme catalysis and ligand binding.

**Acknowledgment.** We are grateful for the support of the NIH (GM-29072) in this work. This work was greatly aided by the receipt of yeast TIM coordinates from G. Petsko, by the receipt of preprints from T. Alber and G. Petsko which greatly aided the model building of the TIM-DHAP complex, and by stimulating conversations with Alber and Petsko. One of us (P.A.K.) thanks Prof. D. C. Phillips of the Oxford Molecular Biophysics Lab for stimulating his interest in TIM while P.A.K. was on sabbatical at Oxford in 1978-79. We also gratefully acknowledge the facilities of the Computer Graphics Lab supported by NIH-RR-

1081, R. Langridge, and T. Ferrin, system manager, which was essential to this research.

**Registry No.** Ia, 57-04-5; Ib, 116-09-6; Ic, 141-46-8; IIIa, 89999-77-9; IIIb, 7333-03-1; IIIc, 1571-60-4; VIIb, 598-35-6; TIM, 9023-78-3; formic acid, 64-18-6.

**Supplementary Material Available:** Listings of structures and energies for  $\alpha$ -hydroxyacetone, its enediolate anion, and glyceraldehyde 3-phosphate (Tables I-III), 4-31G geometry and corresponding energies at the STO-3G and 4-31G levels of HCOO<sup>-</sup> and HCOOH (Table IV), model calculations on anion-neutral complexes (Table V), transition-state II geometry at the 4-31G level (Table VII), and geometries for structures III and V and for transition-state IV at the 4-31G level (Table XI) (7 pages). Ordering information is given on any current masthead page.

## Vinyl Mobility in Myoglobin as Studied by Time-Dependent Nuclear Overhauser Effect Measurements

S. Ramaprasad, Robert D. Johnson,<sup>1</sup> and Gerd N. La Mar\*

Contribution from the Department of Chemistry, University of California, Davis, California 95616. Received July 28, 1983

**Abstract:** Nuclear overhauser effect experiments were performed on the protons of the 2-vinyl group in metcyanomyoglobin. Truncated NOE data were presented, with the observed cross-relaxation rate showing significant vinyl mobility relative to the heme. Good agreement between the selective  $T_1$  rate was found for the 2-H(cis) vinyl resonance, and the effect of cross relaxation on the nonselective  $T_1$  rate is discussed.

The vinyl substituents on the ubiquitous protoheme (A), found as the prosthetic group in myoglobins, hemoglobins, as well as several other classes of hemoproteins,<sup>2</sup> have been implicated in a number of functional roles. In the cases of the oxygen-binding proteins, variable vinyl interactions with the protein have been invoked to account for the Bohr effect in monomeric hemoglobin<sup>3</sup> and have been proposed to play a crucial role in the mechanism of cooperativity in human hemoglobin.<sup>4,5</sup> Interactions between the protein and the heme periphery influence both the equilibrium orientation and the oscillatory mobility of the vinyl group relative to the heme plane. While single-crystal X-ray studies have sometimes differentiated between rotationally locked and rotationally disordered vinyl groups,<sup>6</sup> they generally provide no direct information on the dynamics of this side chain. It can be expected that the oscillatory mobility of the vinyl group will provide a very sensitive probe of heme-protein interactions.

We have been interested in determining by solution NMR methods both the equilibrium orientation and the rotational mobility of heme side chains and the relationship of these properties to protein function. As a model we have selected sperm whale myoglobin in the metcyano form for the initial studies. This protein has been crystallographically characterized in many forms.<sup>6-8</sup> Extensive deuteration studies have provided unequivocal

assignment of many of the hyperfine shifted heme resonances in the <sup>1</sup>H NMR spectrum, including all three protons of the 2-vinyl group.<sup>9,10</sup>

Two NMR methods appear particularly attractive for characterizing the internal motion of heme substituents. It has been shown elsewhere that <sup>2</sup>H NMR relaxation data of isotope-labeled vinyl and propionate side chains can be analyzed in terms of the internal motions.<sup>11,12</sup> Although it is generally thought that paramagnetically shifted or relaxed protons do not exhibit a nuclear Overhauser effect, NOE, because of the sizable paramagnetic "leakage", several cases have been found where cross relaxation, and hence NOEs, contribute significantly to the overall relaxation rate of protons in the heme cavity of a paramagnetic hemoprotein.<sup>13,14</sup> Cross relaxation is also manifested in the curvature of semilogarithmic plots of spin-lattice relaxation experiments,<sup>15</sup> but it can be measured more effectively through the NOE.

The basic NOE experiment is to saturate a specific NMR resonance and observe resultant intensity changes in other resonances that occur through cross relaxation.<sup>16</sup> As the strength

(7) Takano, T. *J. Mol. Biol.* **1977**, *110*, 537.

(8) Phillips, S. E. V. *J. Mol. Biol.* **1980**, *142*, 531.

(9) Krishnamoorthi, R. Ph.D. Dissertation, University of California, Davis, CA, 1983.

(10) Sheard, B.; Yamane, T.; Shulman, R. G. *J. Mol. Biol.* **1970**, *53*, 35.

(11) Johnson, R. D.; La Mar, G. N., submitted for publication; La Jolla Symposium on Protein and Nucleic Acid Structure and Dynamics, La Jolla, CA, September 1982, Abstracts.

(12) Lee, R. W. K.; Oldfield, E. *J. Mol. Biol.* **1982**, *257*, 5023.

(13) Trehwella, J.; Wright, P.; Appleby, C. A. *Nature (London)* **1980**, *280*, 87-88.

(14) La Mar, G. N.; Ramaprasad, S.; McLachlan, S., unpublished results.

(15) Sletten E.; Jackson, J. T.; Burns, P. D.; La Mar, G. N. *J. Magn. Reson.* **1983**, *52*, 492.

(16) Noggle, J. H.; Shirmer, R. E. "The Nuclear Overhauser Effect"; Academic Press: New York, 1971.

(1) Present address, IBM Instruments, Orchard Park, Danbury, CT 08610.

(2) Antonini, E.; Brunori, M. "Hemoglobin and Myoglobin in their Reactions with Ligands", American Elsevier Publishing Co.: New York, 1971; Chapters 4 and 13.

(3) La Mar, G. N.; Viscio, D. B.; Gersonde, K.; Sick, H. *Biochemistry* **1978**, *17*, 361.

(4) Gelin, B. R.; Karplus, M. *Proc. Natl. Acad. Sci. U.S.A.* **1977**, *80*, 1.

(5) Perutz, M. F. *Br. Med. Bull.* **1976**, *32*, 195.

(6) Seybert, D. W.; Moffat, K. *J. Mol. Biol.* **1976**, *106*, 895.

of the NOE depends on the motion of the proton-proton internuclear vector, as well as on the inverse sixth power of the internuclear distance, both structural and dynamical information can be obtained from NOE studies. However, the analysis of steady-state NOEs in proteins is not straightforward, since cross relaxation interconnects all spins in the molecule necessitating a multispin treatment. This problem can be avoided by observing the NOE after short times of saturation (truncated NOE<sup>17</sup>), when the transfer of saturation has affected only the protons close to the saturated proton, and a two-spin approximation may be applied.<sup>18-22</sup> By this method accurate values of cross-relaxation rates are obtained.

We report herein on truncated NOE and spin-lattice relaxation experiments on the 2-vinyl protons of sperm whale metMbCN. By analysis of the cross-relaxation rate  $\sigma$ , in conjunction with the known structure of the vinyl group, we demonstrate how the truncated NOE experiment permits determination of the internal motion of the vinyl group.

### Principles

The time dependence for the magnetization of a proton spin  $I$  is<sup>16,22</sup>

$$I = -\rho_I[I(t) - I(0)] - \sum_k \sigma_{Ik}[K(t) - K(0)] \quad (1)$$

The summation is over all protons in the protein which interact with spin  $I$  through the cross-relaxation terms,  $\sigma_{Ik}$ , with

$$\sigma_{Ik} = \frac{\hbar^2 \gamma_H^4}{20r_{Ik}^6} [6J(2\omega_0) - J(0)] \quad (2)$$

The cross-relaxation terms are measures of the interproton vector  $r_{Ik}$ . The spectral densities,  $J(\omega)$ , are functions of the vector's rotational correlation time and the Larmor frequency,  $\omega_0$ . In a paramagnetic protein, the intrinsic spin-lattice rate of spin  $I$ ,  $\rho_I$ , has two components—a paramagnetic term ( $\rho_{para}$ ), and the usual diamagnetic dipole-dipole terms—and is given by

$$\rho_I = \rho_{para} + \sum_{k \neq I} \frac{\hbar^2 \gamma^4}{20r_{Ik}^6} [J(0) + 3J(\omega_0) + 6J(2\omega_0)] \quad (3)$$

The NOE experiment is to saturate some spin  $k$  and observe its effect on spin  $I$ . The NOE is defined as

$$\eta_I = (I - I_0) / I_0 \quad (4)$$

where  $I$  and  $I_0$  are the intensities with and without saturating spin  $k$ . Saturation of  $k$  alters the magnetization of  $I$  via cross relaxation, as the spins interact through  $\sigma_{Ik}$ . Under the conditions of the truncated NOE experiment, the time dependence of the NOE of peak  $I$ , as a function of the time of saturation,  $t$ , of a peak  $k$ , is given by

$$\eta_I(t) = \frac{\sigma_{Ik}}{\rho_I} (1 - e^{-\rho_I t}) \quad (5)$$

By observing the NOE as a function of  $t$ , an accurate value of the cross-relaxation rate  $\sigma_{Ik}$  is obtained whose analysis through eq 2 yields dynamics information.

The vinyl group, with only three protons, is particularly suitable for a NOE study. The largest NOE will be that between the  $\beta$  cis and trans protons. The simplest NOE experiment is to saturate the 2- $H_\beta$ (trans) and observe the NOE on the 2- $H_\beta$ (cis); the saturation pulse will not significantly affect the 2- $H_\alpha$  proton. The

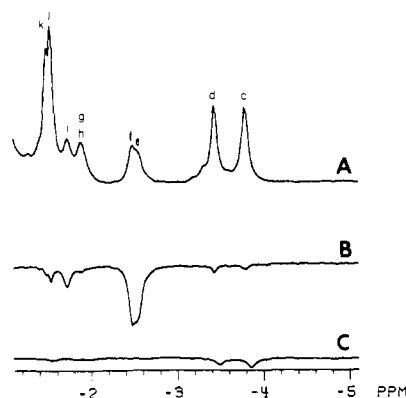
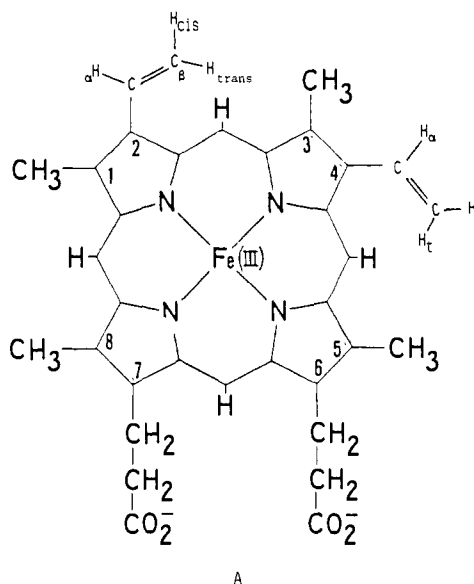


**Figure 1.** Upfield portion of the 360-MHz  $^1\text{H}$  NMR spectra of sperm whale metMbCN in  $^2\text{H}_2\text{O}$ , "pH" 8.5, 25  $^\circ\text{C}$ , and 0.2 M NaCl. (A) Reference spectrum. Peak i has been assigned to the 2- $H_\beta$ (cis) and peak e of composite peak e, f to 2- $H_\beta$ (trans). (B) Steady-state saturation of composite peak e, f showing a NOE to peak i and decoupler spillages to peaks k, j and c, d; vertical scale  $\times 2$  relative to A. (C) The decoupler is positioned at e, -4.8 ppm, showing spillage to peaks c and d; vertical scale  $\times 2$  relative to A.

geometry of the vinyl group being known, the cross-relaxation rate between trans and cis  $H_\beta$ s may be analyzed to obtain the rotational correlation times of the vinyl group, which then will yield data on the dynamics of the cis-trans interproton vector. Thus the mobility of the 2-vinyl group can be characterized.



### Experimental Section

Sperm whale myoglobin was purchased from Sigma Chemical Co. (M-0380) and used without further purification. Metcyanomyoglobin samples were prepared by adding a 4-fold excess of KCN to a 3 mM myoglobin solutions in 0.2 M NaCl in  $^2\text{H}_2\text{O}$ . The pH was adjusted by addition of 0.1 M NaOH or 0.1 M  $^2\text{HCl}$ ; solutions were centrifuged before being transferred to 5-mM NMR tubes. The pH was measured with a Beckman 3550 pH Meter equipped with an Ingold 620 micro-combination electrode; pH values were uncorrected for isotope effect and are referred to as "pH". Chemical shifts are referenced to DSS (2,2-dimethyl-2-sila-5-pentanesulfonate) through the residual water resonance.

Proton NMR spectra were recorded on a Nicolet 360-MHz spectrometer, using 8K data points over a 10-KHz bandwidth. Time-dependent NOE spectra were taken by using the truncated NOE pulse sequence.<sup>17</sup> Saturation pulse lengths varied from 30 to 300 ms; delays between the same were 0.7 s. For a given saturation length, two spectra were recorded—the first with the saturation pulse on the resonance and the second with the saturation pulse off-set by 3000 Hz to provide a reference for the difference spectrum. For each spectrum 1600 scans were collected; difference spectra were analyzed by area. NOE experiments were repeated to verify accuracy.  $T_1$  measurements were performed by using the inversion-recovery method with composite inversion pulses<sup>23</sup> and phase alternation;<sup>24</sup> delays between scans were maintained

(17) Wagner, G.; Wüthrich, K. *J. Magn. Reson.* **1979**, *33*, 675.

(18) Bothner-By, A. A.; Noggle, J. H. *J. Am. Chem. Soc.* **1979**, *101*, 5152.

(19) Olejniczak, E. T.; Poulsen, F. M.; Dobson, C. M. *J. Am. Chem. Soc.* **1981**, *103*, 6574.

(20) Dobson, C. M.; Olejniczak, E. T.; Poulsen, F. M.; Ratcliffe, R. G. *J. Magn. Reson.* **1976**, *21*, 43.

(21) Gordon, S.; Wüthrich, K. *J. Am. Chem. Soc.* **1978**, *100*, 7094.

(22) Solomon, I. *Phys. Rev.* **1955**, *99*, 559.

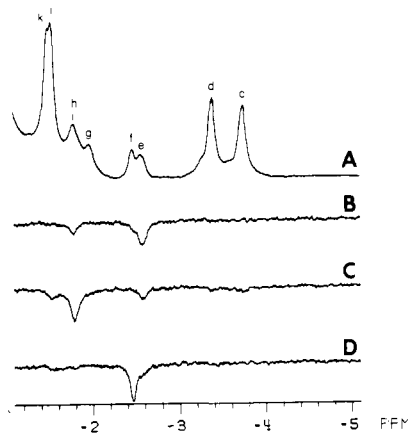


**Figure 2.** Upfield portion of the 360-MHz  $^1\text{H}$  NMR spectra of metMbCN in  $^2\text{H}_2\text{O}$ , "pH" 10.4 25  $^\circ\text{C}$ , and 0.2 M NaCl. (A) Reference spectrum, resolving peak e ( $2\text{-H}_\beta(\text{trans})$ ), but with peak i ( $2\text{-H}_\beta(\text{cis})$ ) merged with peak h. (B) Saturation of peak e, showing a NOE to composite peak h, i. (C) Saturation of composite peak h, i showing a NOE to peak e. (D) Saturation of peak f, showing an absence of NOE to other peaks. Vertical scale  $\times 2$  for B, C, and D relative to A.

at 1.2 s. Selective  $T_1$  measurements were made by using the decoupler for the selective inversion pulse. Care was taken to minimize perturbation of neighboring resonances.

## Results

**Identification of Connected Residues.** The upfield portion of the 360-MHz  $^1\text{H}$  NMR spectrum of sperm whale metMbCN at "pH" 8.5 is shown in A of Figure 1. A combination of variable temperature and pH has led to the identification of nine individual resonances in the spectral window  $-1.2$  to  $-5$  ppm, which are labeled c-k, with c, d, j, and k each arising from a methyl group, with the remaining five peaks being single-proton resonances. Previous isotope labeling and decoupling experiments identified i and e as arising from the 2-vinyl  $\text{H}_\beta(\text{cis})$  and  $\text{H}_\beta(\text{trans})$ , respectively. At "pH" 8.5, peak e is coincident with a protein peak f. The two vinyl peaks of interest, however, are not simultaneously resolved at any pH at 25  $^\circ\text{C}$ , necessitating NOE measurements at two pH values. From the pH behavior outlined in detail elsewhere,<sup>9</sup> the resonances at 10.4 appear as shown in A of Figure 2, where e is now clearly resolved but h as moved on top of i.

Connectivities of the resonances can be established by simple steady-state NOE experiments. Saturating the composite peak e, f in B of Figure 1 leads to the difference spectrum which exhibits a  $-28\%$  NOE only for peak i (see below). The small peaks in trace B from peaks k, j, and c, d arise from decoupler spillage, as verified in the difference trace in C of Figure 1 where the decoupler is set at 4.8 ppm. Thus saturating composite peak e, f leads to a NOE only for peak i in the spectral window of interest. In Figure 2B we display the difference spectrum when the resolved peak e is partially saturated; a NOE is observed for i, h, but must arise only from i. When f is saturated, there is a zero difference spectrum for all other peaks (C in Figure 2), clearly demonstrating that there is a NOE connectivity among the resonances in the window  $-1.6$  to  $-5$  ppm involving exclusively the 2-vinyl  $\text{H}_\beta(\text{trans})$  peak e and the  $2\text{-H}_\beta(\text{cis})$  peak i.

**Truncated NOE and Vinyl Mobility.** The NOE on the  $2\text{-H}_\beta(\text{cis})$  proton of metMbCN was measured after saturating the  $2\text{-H}_\beta(\text{trans})$  proton for various times. The plot of the  $2\text{-H}_\beta(\text{cis})$  NOE vs.  $2\text{-H}_\beta(\text{trans})$  saturation time is shown in Figure 3. The data in Figure 3 show that NOE building up in an exponential fashion, approaching a limiting value of  $-28\%$  after saturation times longer than 200 ms. The calculated NOE at  $t = \infty$  agrees well with the steady-state NOE value, providing justification for the two-spin approximation for this vinyl fragment. Fitting the truncated NOE

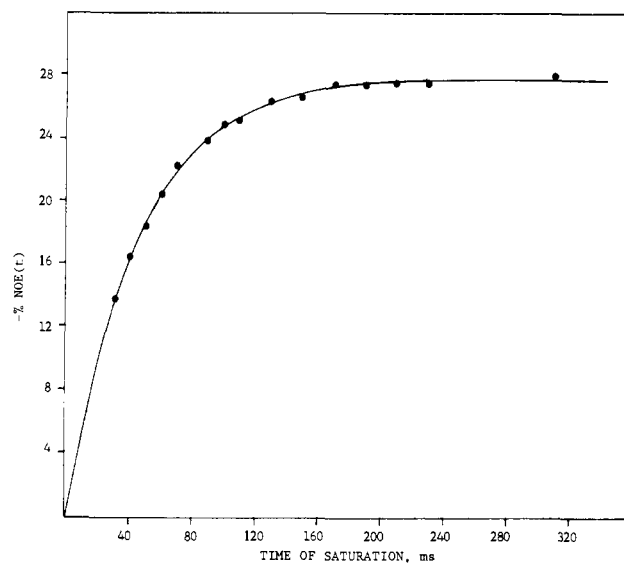


**Figure 3.** Plot of time-dependent NOE of  $2\text{-H}_\beta(\text{cis})$  vs. time saturation of  $2\text{-H}_\beta(\text{trans})$ . Analysis of these data via eq 5 in the text yields  $\sigma(\text{cis-trans}) = -6.1$  Hz and  $\rho_{\text{cis}} = 21.6$  s.

data to eq 5 yields the cross-relaxation rate of  $\sigma(\text{cis-trans}) = -6.1$   $\text{s}^{-1}$  and  $\rho_{\text{cis}} = 21.6$   $\text{s}^{-1}$  (i.e.,  $T_1 = 46$  ms). The fit shows no systematic discrepancies and is insensitive to the omission of the initial or final data points. Both the cross-relaxation rate and  $T_1$  rate exhibit features of interest.

The cis-trans cross-relaxation rate may be calculated for an immobilized vinyl group via eq 2; the spectral densities are then simply

$$J(\omega) = \frac{2\tau_m}{1 + \omega^2\tau_m^2} \quad (6)$$

where  $\tau_m$  is the rotational correlation time of the protein. A variety of techniques have been used to determine  $\tau_m$  for myoglobin, such as  $\gamma\text{-}\gamma$  correlation spectroscopy<sup>26</sup> and  $^2\text{H}$  NMR,<sup>27</sup> yielding a value of 11 ns at 25  $^\circ\text{C}$ . With use of this value for  $\tau_m$  and by setting  $r = 1.88$   $\text{\AA}$ ,<sup>28</sup>  $\sigma(\text{cis-trans}) = -14$   $\text{s}^{-1}$  for an immobilized vinyl. The smaller observed relaxation rate compared to that computed indicates that significant vinyl mobility is present.

The structure of the heme and its vinyl substituents has been well characterized by crystallographic methods.<sup>5-7,28</sup> The vinyls are precluded from being coplanar with the heme due to steric interactions with the heme methyl and meso protons, and two contrasting models have been used to describe internal mobility of such groups. The two-site exchange model<sup>29</sup> assumes a preferred (non-coplanar) orientation of the vinyl and heme planes, with  $180^\circ$  hops between sites at a rate faster than  $\tau_m^{-1}$ . The applicable equation for the rotational correlation time,  $\tau_c$ , is given by

$$\tau_c = \frac{1}{2}J(0) = (1 - \frac{3}{4}\sin^2 2\theta)\tau_m + \frac{3}{4}(\sin^2 2\theta)\frac{\tau_i\tau_m}{\tau_m + \tau_i} \quad (7)$$

with  $\tau_i$  as the site lifetime and  $\theta = 37^\circ$  as the constant angle that  $r(\text{cis-trans})$  makes to the axis of internal rotation;<sup>6,7,28</sup>  $J(2\omega_0)$  is negligible at high fields. The observed  $\sigma$  applied to eq 7 yields  $\tau_i = 2.5$  ns for the two-site model.

The second limiting case simply allows for rotational diffusion of the vinyl group of  $\pi\Omega$  radians from the vinyl position perpendicular to the heme plane;<sup>30</sup>  $180^\circ$  flips occur at a rate slow

(25) La Mar, G. N., unpublished results.

(26) Marshall, A. G.; Lee, K. M.; Martin, P. W. *J. Am. Chem. Soc.* **1980**, *102*, 1460.

(27) Johnson, R. D. Ph.D. Thesis, University of California, Davis, CA, 1983.

(28) Caughey, W. S.; Ibers, J. A. *J. Am. Chem. Soc.* **1977**, *99*, 6639.

(29) Woessner, D. E. *J. Chem. Phys.* **1962**, *36*, 1. Woessner, D. E. *Ibid.* **1961**, *37*, 1. London, R. E. *J. Am. Chem. Soc.* **1978**, *100*, 2678. Wittebort, R. J.; Szabo, A. *J. Chem. Phys.* **1978**, *69*, 1722.

(30) London, R. E.; Avitable, J. *J. Am. Chem. Soc.* **1978**, *100*, 7159. Wittebort, R. J.; Szabo, A. *J. Chem. Phys.* **1978**, *69*, 1722.

(23) Freeman, R.; Kempell, S. P.; Levitt, M. H. *J. Magn. Reson.* **1976**, *38*, 453.

(24) Cutnell, J. D.; Bleich, H. E.; Glasel, S. A. *J. Magn. Reson.* **1976**, *21*, 43.

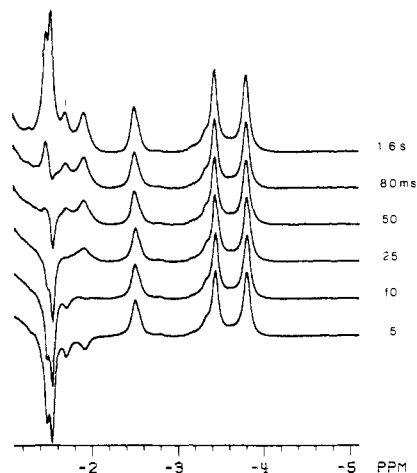


**Figure 4.** Selective  $T_1$  measurement on the 2- $H_{\beta}$ (cis) resonance, peak i, of metMbCN in  $^2H_2O$ , "pH" 8.5 and 25 °C. Peak i has its null point at  $t \sim 38$  ms, yielding an approximate  $T_1$  value of 55 ms.

compared to  $\tau_m$ . Analysis using this model yields the angular range of rotational diffusion. The relevant expression is given by eq 8. The angular range of diffusional motion,  $2\Omega$ , obtained from

$$J(0) = 2\tau_m \left[ \frac{1}{4}(1 - 3 \cos^2 \theta)^2 + \frac{3}{4} \sin^2 2\theta \left[ \frac{(\sin \Omega)/\Omega}{\Omega} \right]^2 + \frac{3}{4} \sin^4 \theta \left[ \frac{(\sin 2\Omega)/2\Omega}{2\Omega} \right]^2 \right] \quad (8)$$

the observed  $\sigma$  is  $\approx 100^\circ$  (i.e., 10% of this angular range lies beyond the heme plane steric barrier). This unrealistically large angular range clearly necessitates another type of motion, presumably jumps across the barrier.  $^2H$  NMR relaxation studies<sup>27</sup> of the mobility of a different vector in the vinyl group show better agreement with the two-site exchange model; however, the assumption of only two sites in the exchange model is also suspect. Further work may allow a more definitive characterization. However, either of these simple models illustrates significant internal rotation of the 2-vinyl group in myoglobin.

**Relaxation Measurements.** The  $T_1$  rate given by eq 3 is directly measurable by a selective  $T_1$  experiment, which was performed on the 2- $H_{\beta}$ (cis) resonance; representative spectra are shown in Figure 4. The null point is determined to be  $\sim 38$  ms by interpolation, yielding a rough estimate of  $T_1(\text{sel}) \sim 55$  ms, in good agreement with the NOE result. The importance of cross relaxation in  $T_1$  measurements can be demonstrated by comparison of these results with the nonselective  $T_1$  experiment. As shown by Granot<sup>31</sup> under nonselective conditions, the initial  $T_1(\text{n sel})$  rate is given by

$$T_1^{-1}(\text{n sel}) = \rho_{\text{para}} + \sum_k \frac{\hbar^2 \gamma_H^4}{20 r_{Ik}^6} [3J(\omega_0) + 12J(2\omega_0)] \quad (9)$$

The  $J(0)$  spectral density terms have canceled out, and as  $J(\omega_0)$  and  $J(2\omega_0)$  are at least an order of magnitude smaller than  $J(0)$  for proteins at high fields, what remains is a reduced relaxation rate that is essentially  $\rho_{\text{para}}$ , the  $T_1$  rate arising from the para-

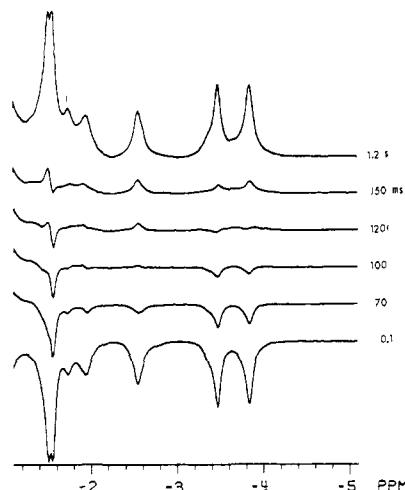


**Figure 5.** Nonselective  $T_1$  measurement of the 2- $H_{\beta}$ (cis) resonance, peak i, for metMbCN in  $^2H_2$ , "pH" 8.5, and 25 °C. Peak i has its null point at  $t \sim 120$  ms, yielding an approximate  $T_1$  value of 180 ms.

magnetic iron. Representative spectra of a nonselective  $T_1$  measurement of the 2- $H_{\beta}$ (cis) resonance are shown in Figure 5. The nonselective  $T_1$  value is  $\sim 180$  ms, corresponding to  $\rho_{\text{para}} = 5.6 \text{ s}^{-1}$ . These results confirm predictions and observations<sup>31-34</sup> made elsewhere. This nonselective  $T_1$  rate, with its paramagnetic origin in iron dipolar relaxation, when compared<sup>35</sup> to heme methyl  $T_1$ 's, confirms that nonselective  $T_1$  measurements are dominated by paramagnetic effects, at least for short times.

In summary, time-dependent NOE studies offer another valuable tool for measuring side-chain mobility in hemoproteins. When accurate molecular tumbling rates are known for a protein, time-dependent NOEs yield cross-relaxation rates that will reveal the extent of internal mobility for the proton-proton vector; these relaxation rates may then be interpreted in terms of motional models. We have shown here that large NOEs exist for hyperfine shifted vinyl peaks in myoglobins and suggest that structure and mobility of other residues in the heme pocket, such as amino acid side chains, can be effectively investigated. Preliminary NOE results indicate that similar structural and dynamic information may be obtained for noncoordinated amino acid side chains in the heme pocket.<sup>36</sup> It may also be anticipated that these methods are applicable to hemoglobin, where variable heme-vinyl contacts are functionally relevant.<sup>4</sup>

**Acknowledgment.** This work was supported by a grant from the National Science Foundation, No. CHE-81-08766.

(31) Granot, J. J. *Magn. Reson.* **1982**, *49*, 257.

(32) Kalk, A.; Berendsen, J. J. C. *J. Magn. Reson.* **1976**, *24*, 343.

(33) Hull, W. E.; Sykes, B. D. *J. Chem. Phys.* **1975**, *49*, 867.

(34) Sloetsz, J. D.; Redfield, A. G. *FEBS Lett.* **1978**, *91*, 320.

(35) Cutnell, J. D.; La Mar, G. N.; Kong, S. B. *J. Am. Chem. Soc.* **1981**, *103*, 3567.

(36) Johnson, R. D.; Ramaprasad, S.; La Mar, G. N. *J. Am. Chem. Soc.* **1983**, *105*, 7205.